Fuzzy Control for a Kite-Based Tethered Flying Robot

Paper:

Fuzzy Control for a Kite-Based Tethered Flying Robot

Yasutake Takahashi*, Tohru Ishii*, Chiaki Todoroki*, Yoichiro Maeda, and Takayuki Nakamura*****

*Department of Human and Artificial Intelligent Systems, Graduate School of Engineering, University of Fukui
3-9-1 Bunkyo, Fukui, Fukui 910-8507, Japan
E-mail: {yasutake, tishii, ctodoroki}@ir.his.u-fukui.ac.jp
**Department of Robotics, Faculty of Engineering, Osaka Institute of Technology
5-16-1 Omiya, Asahi-ku, Osaka 535-8585, Japan
E-mail: maeda@bme.oit.ac.jp
***Faculty of Systems Engineering, Wakayama University
Sakaetani 930, Wakayama 640-8510, Japan
E-mail: ntakayuk@sys.wakayama-u.ac.jp
[Received July 23, 2014; accepted January 29, 2015]

Observation providing information from above is important in in large-scale or dangerous rescue activity. This has been done from balloons or airplanes. Balloon observation requires a gas such as helium and takes a relatively long time to prepare, and while airplane observation can be prepared in a relatively short time and is highly mobile, flight time depends on the amount of fuel a plane can carry. We have proposed and developed a kite-based tethered flying robot that complements balloon and airplane observation while providing a short preparation time and long flight time [1]. The objective of our research is autonomous flight information gathering consisting of a kite, a flight unit, a tether and a ground control unit with a line-winding machine. We propose fuzzy controllers for our robot that are inspired by kite flying.

Keywords: fuzzy control, kite-based flying robot

1. Introduction

Information gathering research and development are done mainly in weather observation [2–5]. Information gathering in large-scale disasters by piloted aircraft has become important because observation from above enables us to collect comprehensive information when it is difficult to move around in the disaster area. Where personnel must stay out of an area, remote-controlled airplanes are often used to gather comprehensive wide-range information. Skilled remote-controlled operation is necessary in controlling remote-controlled airplane safely. A lack of remote-controlled operation skill may cause accidents, so fostering skilled remote operators has become a problem.

Autonomous observation using balloons [6, 7] or airplanes [8–10] has been studied for information gathering from above. Balloons have the advantages of being noise-free and able to stay aloft for a long time, but helium gas must be reserved and relatively long time and gas-maintenance specialists are required. Airplanes need less time for flight preparation, but may be limited by fuel limitations.

While not directly related to information gathering, power generation using kites, balloons, and airplanes has been studied [11, 12]. Yashwanth et al. [13] proposed using a dynamo in a balloon, rotating the balloon with wind and power generation. Balloon-based power generation tends to be large-scale when lifting an electric dynamo. Power generation using kites or airplanes [14–17] must have a certain trajectory for generating electricity by pulling the line connected to a power generator on the ground. Airplane-based power generation requires high-speed flight to pull the line connected to the electric dynamo efficiently and stay in the air. Electricity could be generated during long-term self-contained observation, but systems doing so are not suitable for small-scale stationary observation and information gathering because high-speed high-altitude flight is ill-suited to stationary observation and information gathering.

We have proposed a kite-based tethered flying robot using wind as a natural power source [1] for information gathering complimenting other systems based on balloons or airplanes while having the advantages of short setup and long-term observation. This paper discusses a prototype of the robot we designed and built and its flight systems based on fuzzy controllers inspired by human beings fly kites.

The robot flight unit is controlled by a tether connected to a machine for winding or unwinding the line. The robot has sensors that measure wind speed around the flight unit and its positioning. Robot experiments and computational simulation results confirmed that the fuzzy-based controller carries the kite along autonomously and keeps it stationary in flight.

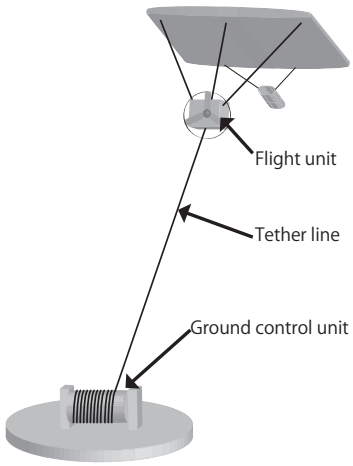

Fig. 1. Tethered flying robot concept.

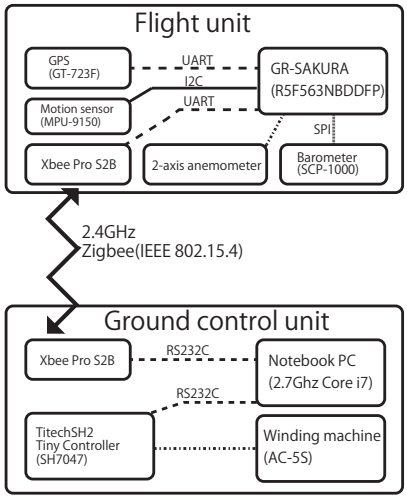

Fig. 2. Schematic robot representation.

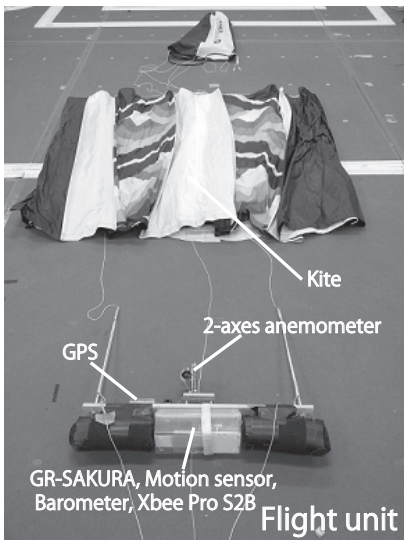

Fig. 3. Flight unit of tethered flying robot.

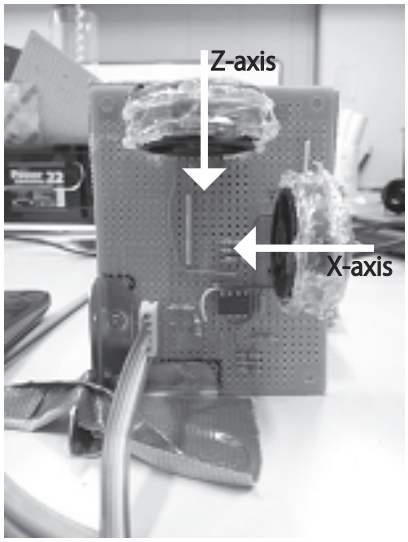

Fig. 4. 2-axis anemometer.

2. System Overview

Our robot consists of a kite, a flight unit, a tether, and a ground control unit, as shown in **Figs. 1** and **2**. The flight unit has sensors and transmits wind status and the flight unit's position and orientation to the ground wirelessly. The flight unit is lifted by the kite. The ground control unit manages the tether to the flight unit based on data from the flight unit. A ZigBee module provides wireless communication between the flight unit and the ground control unit.

2.1. Kite and Flight Unit

The kite wingspan is 3.2 m and its chord is 1.5 m long (**Fig. 3**). The kite weighs about 700 g and carries up to 1500 g in equipment.

The flight unit has anemometers to measure wind speed around the flight unit. It also has a GPS for estimating its own position in the air, a motion sensor that includes an accelerometer and a rate gyroscope for measuring posture of the flight unit, and a ZigBee Xbee Pro S2B module for transmitting wireless data to the ground control unit. It uses a barometer to calculate the flight unit's altitude based on the atmospheric pressure difference from the ground. The GR-SAKURA microcomputer (**Fig. 2**) receives sensor information. The flight unit weighs about 850 g.

The 2-axis anemometer we designed and developed (**Fig. 4**) uses impellers for its commercially available portable anemometers and magnetic encoders. It measures even weak wind because of its very low resistance load. The kite has only one line to be controlled and the flight unit cannot control its posture. The anemometer on the flight unit measures wind speed around the flight unit orthogonally in two directions. When the flight unit is inclined, the wind speed against the flight unit from wind speed is calculated orthogonally in two directions and used for control.

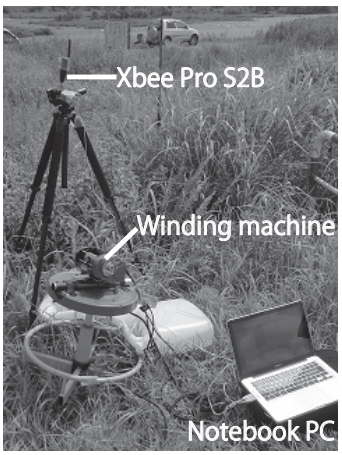

Fig. 5. Ground control unit.

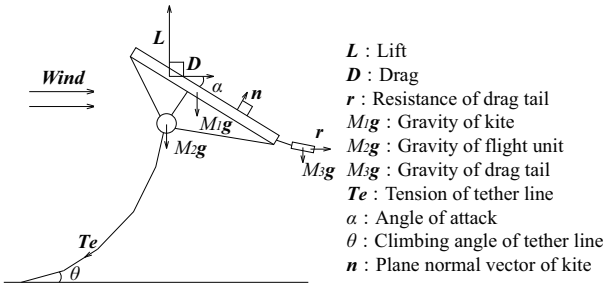

Fig. 6. Model of tethered flying robot.

2.2. Ground Control Unit

The ground control unit we developed (**Fig. 5**) consists of a notebook computer and a line-winding machine. The tether weighs about 37.1 g/100 m. The notebook computer receives data from the flight unit and controls the line-winding machine by using a microcomputer (TitechSH2 Tiny Controller, **Fig. 2**). We used an AC-5S (MIYAMAE Co., Ltd.) originally serving as an electric reel for fishing. We then modified it for line-winding. The line-winding uses an electric clutch to adjust brake force in line release. The encoder in the line-winding machine acquires information, including line length and rotation number. The line to the line-winding machine is about 300 m long. Maximum winding power is 64 kg and maximum winding speed is 2.5 m/s.

3. Robot Model

Our robot's 2D model is shown in **Fig. 6**. A kite may change shape depending on the wind around the kite. Here, however, we assume that the kite changes shape minimally during flight because wind is strong enough to lift the kite itself during flight and keeps the kite's shape as is. The kite is therefore modeled as a board in the dynamics engine simulator. We use Open Dynamics Engine (ODE) [18] for our robot's dynamics simulator. Lift force $\boldsymbol{L}$, drag force $\boldsymbol{D}$, and the point of the forces are modeled

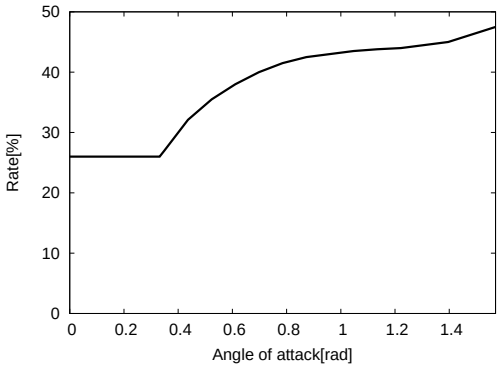

Fig. 7. Position of the working point to the chord length from the leading edge of the chord line.

based on the work of Okamoto et al. [19]. **Fig. 7** shows the points of forces, $\boldsymbol{L}$ and $\boldsymbol{D}$, from the leading edge of the kite. The point of forces is the ratio against the chord length. $\boldsymbol{L}$ and $\boldsymbol{D}$ are calculated using Eqs. (1) and (2).

$$\boldsymbol{L} = \frac{1}{2} C_l \rho S (\boldsymbol{U} \times \boldsymbol{n}) \times \boldsymbol{U} \quad \ldots\ldots\ldots\ldots (1)$$

$$\boldsymbol{D} = \frac{1}{2} C_d \rho S \|\boldsymbol{U}\| \boldsymbol{U} \quad \ldots\ldots\ldots\ldots (2)$$

$$\rho = \frac{1.293P}{1.0 + \dfrac{t}{273.15}} \quad \ldots\ldots\ldots\ldots (3)$$

ρ is air density [kg/m^3] calculated using Eq. (3). P is atmospheric pressure [atm] and t is temperature in Centigrade. $\boldsymbol{U}$ is the relative wind velocity against the kite [m/s], $\boldsymbol{n}$ is the normal vector of the kite plane, and and S is the frontal projected area [m^2]. C_l and C_d, the lift and drag coefficients, depend on attack angle α and the kite wing configuration. In practice, the parameters should be identified using a real wind-tunnel testing, but, it is difficult to conduct such a test using a kite. We, therefore, used Eqs. (4) and (5) based on [20]. Unfortunately, these equations provide parameter values only when attack angle α is from 0 rad to $\pi/4$ rad. Lift coefficient C_l is therefore interpolated linearly while attack angle $\alpha > \pi/4$ under the constraint that $C_l = 0$ when $\alpha = \pi/2$. We assume that drag coefficient C_d changes minimally if attack angle α exceeds $\pi/4$ rad so that C_d when $\alpha > \pi/4$ is the value of C_d when $\alpha = \pi/4$. These assumptions follow the work of Okamoto et al. [19],

$$C_l = \frac{2.0\alpha\pi}{1.0 + \dfrac{2.0\alpha}{A_r}} \quad \ldots\ldots\ldots\ldots (4)$$

$$C_d = 1.28 \sin\alpha + \frac{C_l^2}{0.7\pi A_r} \quad \ldots\ldots\ldots\ldots (5)$$

where A_r is the aspect ratio of the kite wing.

Drag from the kite's drag tail is measured in actual experiments with the drag tail and modeled for use in simulation.

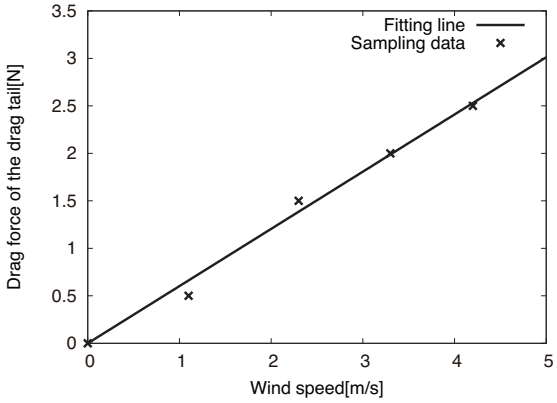

Fig. 8. Experimental results for the relationship between wind speed and drag using an actual kite's drag tail.

Fig. 9. Experimental results of the robot taking off in a windless situation.

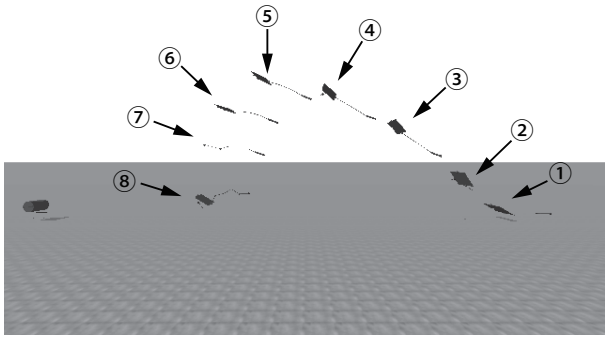

Fig. 10. Results of the computational simulated robot taking off in a windless situation.

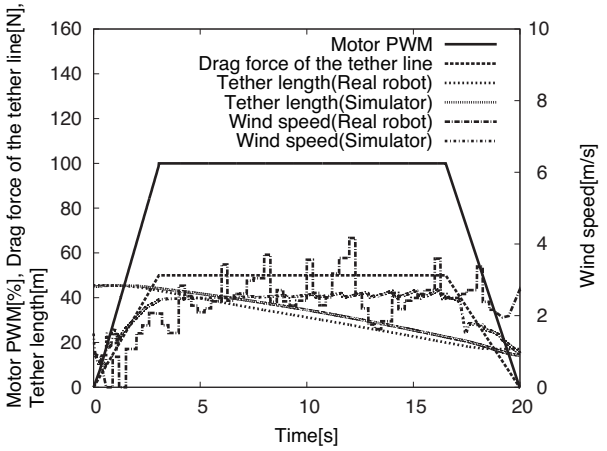

Fig. 11. Control, tether length, and wind speed.

Figure 8 shows the experimental results for the relationship between wind speed and drag force using actual drag tail. Experimental results indicate that drag force r of the drag tail is estimated using the following simple linear equation:

$$r = 0.602341v \quad \ldots\ldots\ldots\ldots\ldots\ldots \quad (6)$$

where v is wind speed. **Fig. 8** shows sampling data and the fitting line indicating the experimental results and Eq. (6).

We assume that the tether consists of a set of 20 small rigid sticks because the ODE does not have a flexible line model. The line connecting the drag tail and the kite is modeled similarly as the tether line using 3 sticks. Each such stick has mass and the simulator takes gravity into account. The line winding of the ground control unit is modeled as dragging of the tether. Note that the ODE does not consider air friction, although, the actual robot is influenced by air friction. The viscous friction of air is therefore added to each rigid body on the ODE in the direction opposite to the air in relative object velocity. In actual experiments, a safety line attached to the flight unit prevents the flight unit from being released if the main tether line is cut. The simulator takes this into consideration, i.e., gravity and viscous wind friction are added to dynamics simulation. The actual robot catches the wind from the side, but the computer simulator does not consider this.

We compared take off flight data from the computer-simulated model and the actual robot at a 1.5 m/s wind speed at ground level. The winding machine controls tether winding and the actual ground control unit control the power with the duty ratio of the PWM module input to the winding motor. The simulated model controls power directly with tether drag. Winding power is increased from 0 to the maximum in the first 3 s, kept as is for 15 s, and then decreased to 0 within 3 s. **Fig. 9** shows take off behavior of the robot in a windless situation for the real robot and **Fig. 10** for the simulation. **Fig. 11** shows motor inputs to the ground control unit, i.e., "Motor PWM" for the real robot and "drag force of the tether line" for the simulated one, tether line length, and wind speed for the flight unit in the real experiment and simulation. **Fig. 12** shows the flight unit altitude. Solid lines indicate the altitudes of the real robot and broken lines the simulated one. Data for the real robot includes sensor noises. Resolution is comparatively low because of the altitude sensor, unfortunately. Even so, simulated flight unit behavior during the flight is similar enough to the real one that the simulator can be used to evaluate flight controller performance.

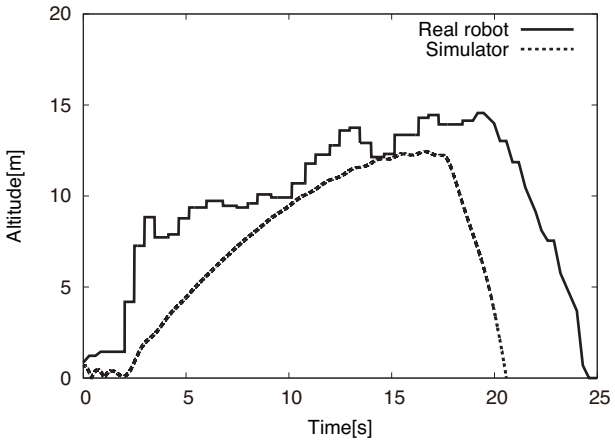

Fig. 12. Comparison of real robot and simulated one altitude.

4. Flying Fuzzy Controller

Our fuzzy controller is inspired by human kite flying. Fuzzy sets reasonably represent unwritten policy that represents such flight. A kite flyer controls kite line based on wind speed, line drag, altitude and kite motion. Here, we design two fuzzy controllers for flight – one of them controlling drag and release based on a fuzzy set of kite altitude and wind speed measured by the flight unit and the other considering altitude change. Fuzzy controllers are represented based on simplified reasoning in Eqs. (7), (8), and (9). Eq. (7) shows the fitness degree calculation for 2 inputs and Eq.(8) that for case of 3 inputs.

$$\begin{aligned} &\text{Rule } i\text{: If } w \text{ is } WS_i \text{ and } a \text{ is } ALT_i \\ &\quad \text{then } \varphi \text{ is } b_i \ (i = 1,2,\ldots,\mathrm{n}) \\ &\quad h_i = \min(\mu_{WS_i}(w), \mu_{ALT_i}(a)) \quad \ldots\ldots\ldots (7) \end{aligned}$$

$$\begin{aligned} &\text{Rule } i\text{: If } w \text{ is } WS_i \text{ and } a \text{ is } ALT_i \text{ and } v_a \text{ is } DALT_i \\ &\quad \text{then } \varphi \text{ is } b_i \ (i = 1,2,\ldots,\mathrm{n}) \\ &\quad h_i = \min(\mu_{WS_i}(w), \mu_{ALT_i}(a), \mu_{DALT_i}(v_a)) \quad . \quad (8) \end{aligned}$$

$$\varphi = \frac{\sum_{i=1}^{n} h_i b_i}{\sum_{i=1}^{n} h_i} \quad \ldots\ldots\ldots\ldots\ldots (9)$$

h_i in Eqs. (7) and (8) indicates the degree of rule i, given wind speed w, altitude a, and altitude change v_a. $\mu_{WS_i}(w)$, $\mu_{ALT_i}(a)$, and $\mu_{DALT_i}(v_a)$ are membership functions corresponding to wind speed, altitude, and altitude change for rule i. Membership functions are shown in **Fig. 13**.

φ in Eq. (9) indicates control input given to the winding machine, calculated as the weighted sum of the consequent singleton of rule i with weight h_i. The singleton is shown in **Fig. 14**. $\varphi = 100$ indicates 100% drag force. $\varphi = -100$ indicates that brake force is zero to release the tether. $\varphi = 0$ indicates that drag is zero and brake force is maximum to keep the tether line length.

Table 1 shows the rule table for the fuzzy controller based on 2 inputs, i.e., wind speed and altitude. The controller tries to drag the line when kite altitude or the wind speed is low. It releases the line if wind speed is high and altitude is medium. If altitude is high enough and wind speed is relatively high, then it tries to keep the line length.

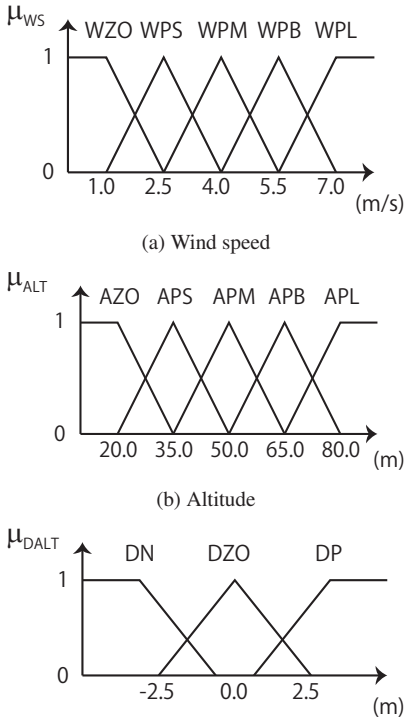

(a) Wind speed

(b) Altitude

(c) Altitude change

Fig. 13. Antecedent membership function.

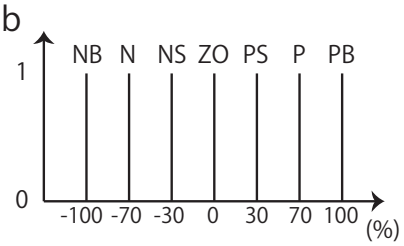

Fig. 14. Consequent singleton.

Table 2 shows the rule table for the fuzzy controller based on 3 inputs, i.e., wind speed, altitude, and change of altitude. The idea concerning the controller is the same as that for the 2 inputs controller in **Table 1** and information on the change in altitude is added. If the kite falls, the controller tends to drag the line to maintain kite altitude as higher as possible. If the kite goes higher, the controller reduces drag and releases the line if possible.

Parameters in **Tables 1** and **2**, membership functions and singletons are designed by hand first and adjusted through trial and error during actrual robot experiments. (In future work, we plan to use the simulation above to tune the parameters.)

4.1. Actually Robot Experiments

Actually robot experiments are conducted to evaluate how fuzzy controllers work in an actual environment. The

Table 1. Fuzzy rule for 2 inputs and 1 output.

		Altitude				
		AZO	APS	APM	APB	APL
Wind speed	WZO	PB	PB	PB	P	NS
	WPS	PB	PB	PB	PS	NS
	WPM	PB	PB	P	ZO	ZO
	WPB	PB	P	PS	ZO	ZO
	WPL	P	NS	NS	ZO	ZO

Table 2. Fuzzy rule for 3 inputs and 1 output.

				Altitude				
				AZO	APS	APM	APB	APL
Wind speed	WZO	Altitude change	DN	PB	PB	PB	PB	PB
			DZO	PB	PB	P	PS	ZO
			DP	PB	P	PS	ZO	ZO
	WPS	Altitude change	DN	P	P	P	PS	PS
			DZO	PS	ZO	ZO	ZO	ZO
			DP	ZO	ZO	ZO	ZO	ZO
	WPM	Altitude change	DN	P	P	PS	PS	PS
			DZO	PS	ZO	NS	ZO	ZO
			DP	ZO	NS	NS	ZO	ZO
	WPB	Altitude change	DN	P	PS	PS	PS	PS
			DZO	NS	NS	NS	ZO	ZO
			DP	N	N	N	ZO	ZO
	WPL	Altitude change	DN	PS	PS	PS	PS	ZO
			DZO	N	N	N	ZO	ZO
			DP	NB	N	N	ZO	ZO

length of the tether between the flight unit and ground control unit is set at about 75 m. At the beginning of flight, the ground control unit winds the tether up to take off the kite and flight unit based on the fuzzy controllers.

Figure 15 shows the flight log for the PWM duty ratio, wind speed, line length, and altitude while the 2 inputs and 1 output for the fuzzy controller with the fuzzy rules in **Table 1** are applied. The PWM duty ratio indicates drag and release to winch the tether, i.e., φ in Eq. (9) is the control input to the line-winding machine. **Fig. 16** shows flight trajectory based on the GPS and barometer output. The cross (GCU) at left in **Fig. 16** indicates the location of the ground control unit.

Figure 15 shows that the flight unit takes off successfully and ascends into the sky because of the high wind speed until about 190 s. The wind suddenly stops from 190 s to 300 s, then the flight unit drops and the ground control unit starts to drag the line. The motor output rises slowly, however, because the flight unit altitude is high. This leads the flight unit to greatly reduce altitude. **Fig. 16** shows flight unit behavior. To avoid undesired altitude loss by the flight unit, the controller requires information both on the wind speed and altitude and on the altitude change of the flight unit.

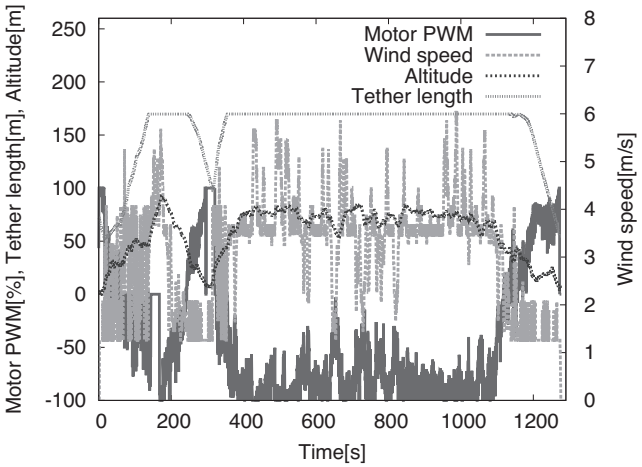

Fig. 15. Flight log (Motor power, Wind speeds, Tethered line length, Altitude) by 2-inputs 1-output fuzzy controller.

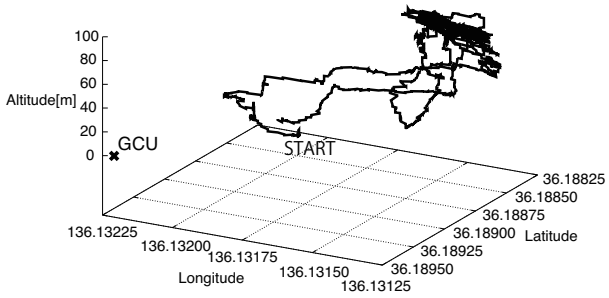

Fig. 16. Flight log (GPS, altitude) by 2-inputs 1-output fuzzy controller.

After it recovers altitude at about 400 s, the ground control unit controls the line to maintain the altitude of the flight unit stably at about 75 m. The wind stops again at about 1100 s and the ground control unit starts to drag the tether, then the flight unit continues to reduce altitude and lands.

Figures 17 and **18** show the flight log for the PWM duty ratio, wind speed, line length and altitude while the 3 inputs and 1 output fuzzy controller with the fuzzy rules in **Table 2** are applied. **Fig. 18** shows the flight log from 0 s to 300 s for **Fig. 17**. When the begins, the ground control unit drags the line to lift the flight unit based on the fuzzy controller. It, then reduces drag based on the wind speed measured by the flight unit and releases the line at about 50 s. Unfortunately, the wind becomes weak

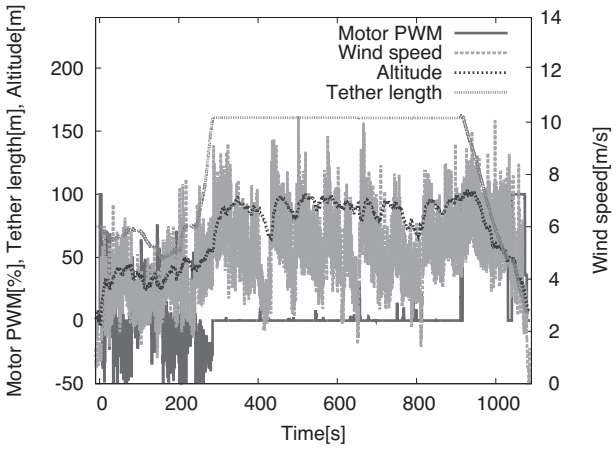

Fig. 17. Flight log for motor power, wind speeds, tethered line length, and altitude during the flight of 3 inputs and 1 output for the fuzzy controller.

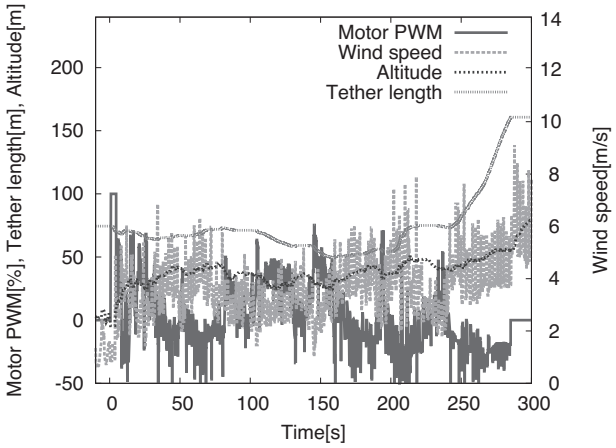

Fig. 18. Flight log for motor power, wind speeds, tethered line length, and altitude during the flight of 3 inputs and 1 output for the fuzzy controller at the beginning of **Fig. 17**.

at about 100 s and 230 s then the ground control unit drags the line to maintain flight unit altitude. The wind becomes strong again at about 200 s and 250 s, then the ground unit reduces drag and releases the line, causing the flight unit altitude to rise higher and higher. After around 250 s, the wind becomes strong enough to lift the flight unit to a high altitude. The ground control unit stops releasing the tether after around 280 s because the maximum tether length is set at 170 m. When the wind becomes weak, the ground control unit tends to increase drag. If the wind becomes strong enough in short time, the line is not actually dragged, but maintains altitude stably from 70 m to 100 m. The line is wound manually from about 920 s to land the flight unit. Winding is interrupted at about 1050 s because the winding machine motor becomes too hot to drag the line safely, although the flight unit finally lands.

Figure 19 shows the flight trajectory based on the GPS and barometer output. The cross (GCU) at left In **Fig. 19** indicates the location of the ground control unit. The flight trajectory shows the flight situation mentioned

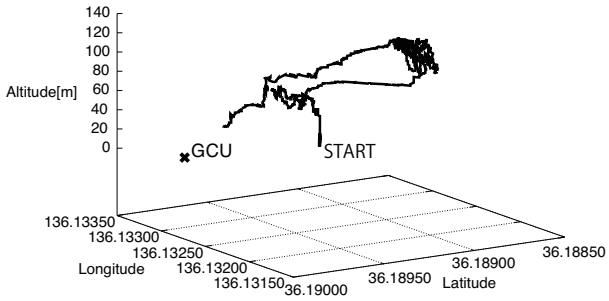

Fig. 19. Flight log for GPS and altitude during the flight of 3 inputs and 1 output for the fuzzy controller.

above. The flight unit rises at the beginning of the flight and stays there while the wind remains weak from 10 s to 250 s. After about 250 s, the wind becomes strong enough to lift the flight unit to a high altitude and the ground control unit releases the line. The flight unit rises until the line reaches its limit, after which, the line is wound manually until the flight unit lands.

As these figures show, the 3 inputs and 1 output of the fuzzy controller works fine in controlling robot successfully.

4.2. Computational Simulation

Computational simulation is conducted to evaluate in detail how the fuzzy controllers work. The length of the tether between the flight unit and ground control unit is set to 60 m, then wind above the ground is generated artificially, based on a sine function. The wind varies in a range from 0 to 4.0 m/s over a period of 20 s.

Figure 20 shows flight logs with and without the proposed 3 inputs and 1 output for the fuzzy controller. The wind speed above the ground is represented by the line labelled "Wind speed (ground)." The label "Wind speed" indicates the wind speed around the flight unit in the figure. **Fig. 20(a)** shows that the fuzzy controller increases the altitude of the flight unit successfully so that it drags the tether when the wind is weak and releases the tether when the wind is strong. **Fig. 20(b)** shows that the flight unit drops to the ground when the wind is weak if the length of the tether is fixed without control. It cannot keep the flight unit in the air stably. **Fig. 20(c)** compares altitude logs for both cases, indicating the feasibility of the fuzzy controller when the wind is weak and how the fuzzy controller controls the flight unit in the same manner as a human being would fly a kite.

5. Conclusions

The objective of this research is to realize a flying observation system that complements other information gathering systems using a balloon or an air vehicle. We proposed a kite-based tethered flying robot with long-term capability, and this paper has shown a mathematical model of the robot, two flight controllers based on fuzzy

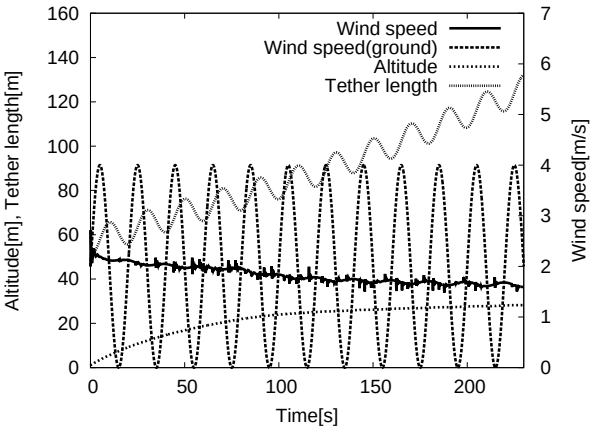

(a) Fuzzy controller

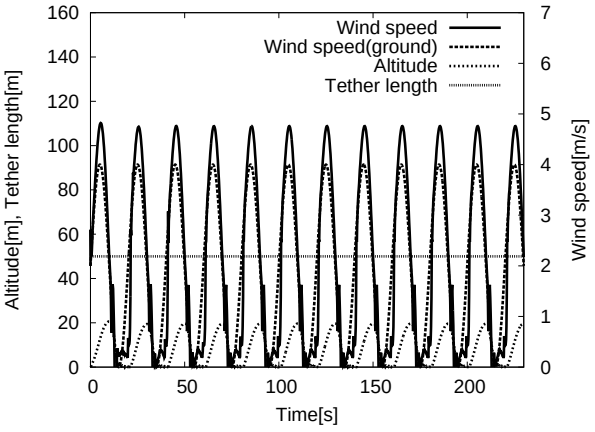

(b) No control

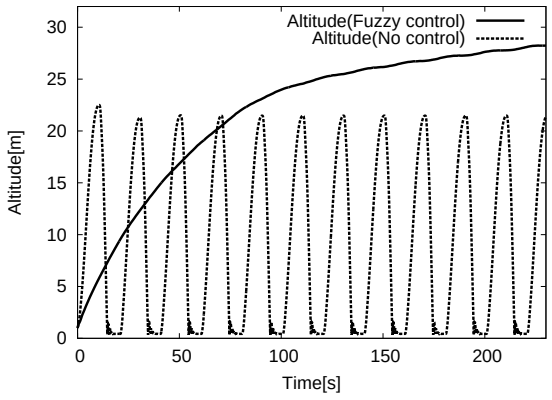

(c) Altitude log

Fig. 20. Comparison of flight behavior with and without the fuzzy controller.

control, and the performance of our methods through actual robot experiments and computational simulation. One of our future objectives is to determine the parameters of fuzzy controllers membership functions and singletons.

Acknowledgements

This work was supported in part by JSPS KAKENHI Grant No. 24650118.

References:

[1] T. Ishii, Y. Takahashi, Y. Maeda, and T. Nakamura, "Tethered flying robot for information gathering system," in IROS'13 Workshop on Robots and Sensors integration in future rescue INformation system (ROSIN'13), 2013.

[2] M. Nishida, T. Katayama, A. Ishii, J. Tsutsumi, and K. Tajima, "Observation of wind profiles in urban area by kytoon," J. of Structural and Construction Engineering, No.365, pp. 10-18, 1986.

[3] N. Hirasawa, "Summary of the atmospheric observation with meteorological sonde and of radiation and cloud at dome fuji station in antarctica and the preliminary results.," TENKI, Vol.46, No.2, pp. 147-152, 1999.

[4] T. Nakao, K. Fujiwara, M. Furukawa, and T. Hiroe, "Development of a compact captive balloon and its level supporting," J. of the Japan Society for Aeronautical and Space Sciences, Vol.53, No.612, pp. 9-14, 2005.

[5] J. Henry M. Cathey and D. L. Pierce, "Development of the nasa ultra-long duration balloon," in NASA Science Technology Conf., Paper C3P2, 2007.

[6] H. Aichi, M. Kumada, T. Kobayashi, Y. Sugiyama, K. Horii, and S. Yokoi, "Application to power generation by wind and environmental watching and/or it system by floating platform tethered with cable, and preliminary study on climbing characteristics of a tethered aerodynamic platform with side-by-side twin rotors," Bulletin of Daido Institute of Technology, Vol.38, pp. 213-223, 2002.

[7] H. Aichi, M. Kumada, T. Kobayashi, Y. Sugiyama, K. Horii, and S. Yokoi, "Application of floating platform tethered with cable in high altitude to wind power generation, telecommnication/broadcasting, and environmental watching," Denkiseiko, Vol.74, No.3, pp. 167-172, 2003.

[8] S. Karim and C. Heinze, "Experiences with the design and implementation of an agent-based autonomous uav controller," in Proc. of the 4th Int. Joint Conf. on Autonomous Agents and Multiagent Systems (AAMAS'05), New York, USA, pp. 19-26, ACM, 2005.

[9] J. Fujinaga, H. Tokutake, and S. Sunada, "Guidance and control of a small unmanned aerial vehicle and autonomous flight experiments," J. of the Japan Society for Aeronautical and Space Sciences, Vol.56, No.649, pp. 57-64, 2008.

[10] T. Suzuki, J. Meguro, Y. Amano, T. Hashizume, D. Kubo, T. Tsuchiya, S. Suzuki, R. Hirose, K. Tatsumi, K. Sato, and J. Takiguchi, "Development of information collecting system using a small unmanned aerial vehicle for disaster prevention and mitigation," J. of Robotics Society of Japan, Vol.26, No.6, pp. 553-560, 2008.

[11] W. Engels, T. Obdam, and F. Savenije, "Current developments in wind," Tech. Rep. ECN-E-09-96, Energy research center of the Netherlands, 2009.

[12] M. Canale, L. Fagiano, and M. Milanese, "Power Kites for Wind Energy Generation – Fast Predictive Control of Tethered Airfoils," IEEE Control Systems Magazine, pp. 25-38, 2007.

[13] P. Yashwanth, P. V. Ganesh, E. Arunprakash, and S. Benisha, "Floating power station (mars the future wind-mill)," IOSR J. of Electrical and Electronics Engineering, Vol.2, No.1, pp. 10-13, 2012.

[14] B. Landorp and P. Williams, "The laddermill: Innovative wind energy from high altitudes in holland and australia," Windpower 06, 2006.

[15] B. Lansdorp, R. Ruiterkamp, and W. Ockels, "Towards flight testing of remotely controlled surfkites for wind energy generation," AIAA Atmospheric Flight Mechanics Conference and Exhibit, Vol.6643, No.August, 2007.

[16] B. Houska and M. Diehl, "Robustness and stability optimization of power generating kite systems in a periodic pumping mode," 2010 IEEE Int. Conf. on Control Applications, pp. 2172-2177, 2010.

[17] I. Argatov and R. Silvennoinen, "Energy conversion efficiency of the pumping kite wind generator," Renewable Energy, Vol.35, No.5, pp. 1052-1060, 2010.

[18] R. Smith, "Open dynamics engine," 2008. http://www.ode.org/.

[19] T. Okamoto, M. Fujisawa, and K. T. Miura, "Development of a user inteactive kite simulation system," Graphics and CAD/Visual Computing Joint Symp. 2009, 2009 (in Japanese).

[20] "NASA Kite Modeler 1.5a." http://www.grc.nasa.gov/WWW/K-12/airplane/kiteprog.html, 2008. [Online; Accessed November 7, 2013]

Name:
Yasutake Takahashi

Affiliation:
Department of Human and Artificial Intelligent Systems, Graduate School of Engineering, University of Fukui

Address:
3-9-1 Bunkyo, Fukui, Fukui 910-8507, Japan

Brief Biographical History:
2000-2009 Assistant Professor of Department of Adaptive Machine Systems, Graduate School of Engineering, Osaka University
2006-2007 Visiting researcher at the Fraunhofer IAIS
2009-2012 Senior Assistant Professor of Department of Human and Artificial Intelligent Systems, Graduate School of Engineering, University of Fukui
2012- Associate Professor of Department of Human and Artificial Intelligent Systems, Graduate School of Engineering, University of Fukui

Main Works:
• Y. Takahashi, K. Noma, and M. Asada, "Efficient Behavior Learning based on State Value Estimation of Self and Others," Advanced Robotics, Vol.22, No.12, pp. 1379-1395, 2008.
• Y. Takahashi, Y. Tamura, M. Asada, and M. Negrello, "Emulation and Action Understanding through Shared Values," ROBOTICS AND AUTONOMOUS SYSTEMS J., Vo.58, No.7, pp. 855-865, 2010.
• Y. Tamura, Y. Takahashi, and M. Asada, "Observed Body Clustering for Imitation Based on Value System," J. of Advanced Computational Intelligence and Intelligent Informatics, Vol.14, No.7, pp. 802-812, 2010.

Membership in Academic Societies:
• The Robotics Society of Japan (RSJ)
• Japan Society for Fuzzy Theory and Intelligent Informatics (SOFT)
• The Japanese Society for Artificial Intelligence (JSAI)
• The Institute of Electrical and Electronics Engineers (IEEE)

Name:
Tohru Ishii

Affiliation:
Department of Human and Artificial Intelligent Systems, Graduate School of Engineering, University of Fukui

Address:
3-9-1 Bunkyo, Fukui, Fukui 910-8507, Japan

Brief Biographical History:
2010-2012 Faculty of Engineering, University of Fukui
2012-2014 Graduate School of Engineering, University of Fukui
2014- Advanced Defense Technology Center, Technical Research and Development Institute, Ministry of Defense

Main Works:
• T. Ishii, Y. Takahashi, Y. Maeda, and T. Nakamura, "Fuzzy Control for Kite-based Tethered Flying Robot," Proc. of 2014 IEEE Int. Conf. on Fuzzy Systems, Vol.CD-ROM, pp. 746-751, 2014.

Name:
Chiaki Todoroki

Affiliation:
Department of Human and Artificial Intelligent Systems, Graduate School of Engineering, University of Fukui

Address:
3-9-1 Bunkyo, Fukui, Fukui 910-8507, Japan

Brief Biographical History:
2010-2014 Faculty of Engineering, University of Fukui
2014- Graduate School of Engineering, University of Fukui

Main Works:
• C. Todoroki, Y. Takahashi, and T. Nakamura, "Learning Fuzzy Control Parameters for Kite-based Tethered Flying Robot using Human Operation Data," Proc. of Joint 7th Int. Conf. on Soft Computing and Intelligent Systems and 15th Int. Symp. on Advanced Intelligent Systems, pp. 111-116, 2014.

Membership in Academic Societies:
• Japan Society for Fuzzy Theory and Intelligent Informatics (SOFT)

Name:
Yoichiro Maeda

Affiliation:
Department of Robotics, Faculty of Engineering, Osaka Institute of Technology

Address:
5-16-1 Omiya, Asahi-ku, Osaka 535-8585, Japan

Brief Biographical History:
1983- Researcher, Central Research Lab., Mitsubishi Electric Corp.
1989-1992 Senior Researcher, Laboratory for International Fuzzy Engineering Research (LIFE)
1995- Associate Professor, Osaka Electro-Communication University
1999-2000 Visiting Researcher, University of British Columbia (UBC)
2002- Associate Professor, Faculty of Engineering, University of Fukui
2007- Professor, Graduate School of Engineering, University of Fukui
2013- Professor, Faculty of Engineering, Osaka Institute of Technology

Main Works:
• Y. Maeda, M. Tanabe, and T. Takagi, "Behavior-Decision Fuzzy Algorithm for Autonomous Mobile Robots," Information Sciences, Vol.71, No.1, pp. 145-168, 1993.
• Y. Maeda, "Emotional Generation Model for Autonomous Mobile Robot," KANSEI Engineering Int., Vol.1, No.1, pp. 59-66, 1999.
• Y. Maeda and Y. Kajihara, "Automatic Generation of Musical Tone Row and Rhythm Based on the Twelve-Tone Technique Using Genetic Algorithm," J. of Advanced Computational Intelligence and Intelligent Informatics (JACIII), Vol.14, No.3, pp. 288-296, 2010.

Membership in Academic Societies:
• The Society of Instrument and Control Engineers (SICE)
• The Robotics Society of Japan (RSJ)
• Japan Society for Fuzzy Theory and Intelligent Informatics (SOFT)
• The Japanese Society for Artificial Intelligence (JSAI)
• Japan Society of Kansei Engineering (JSKE)

Name:
Takayuki Nakamura

Affiliation:
Department of Computer and Communication Sciences, Wakayama University

Address:
930 Sakaedani, Wakayama 640-8510, Japan

Brief Biographical History:
1996- Visiting Researcher, Brown University Computer Science
1997- Research Associate, Nara Institute of Science and Technology
2002- Associate Professor, Wakayama University
2007- Visiting Researcher, Carnegie Mellon University Robotics Institute
2013- Professor, Wakayama University

Main Works:
• T. Nakamura, T. Kato, and T. Wada, "A Novel Non Linear Mapping Algorithm (PaLM-Tree)," J. of Robotics Society of Japan, Vol.23, No.6, pp. 732-742, 2005 (in Japanese).

Membership in Academic Societies:
• The Robotics Society of Japan (RSJ)